Optimizing Comprehensive Cost of Charger Deployment in Multi-hop Wireless Charging

SIXU WU and LIJIE XU, Jiangsu Key Laboratory of Big Data Security and Intelligent Processing, Nanjing University of Posts and Telecommunications, China
HAIPENG DAI, The State Key Laboratory for Novel Software Technology, Nanjing University, China
LINFENG LIU, FU XIAO, and JIA XU*, Jiangsu Key Laboratory of Big Data Security and Intelligent Processing, Nanjing University of Posts and Telecommunications, China

The multi-hop wireless charging technology has attracted a lot of attention as it largely extends the charging range of chargers. Different from the existing work with single cost optimization, the objective of this paper is to optimize the comprehensive cost, which is the combination of energy cost and deployment cost. We decompose the target problem into two sub-problems. The first sub-problem aims to minimize the deployment cost with energy capacity constraints. The proposed algorithm follows the greedy strategy, where the subset of sensor nodes for any charger is determined by finding the capacitated minimum spanning tree. The second sub-problem, which aims to maximize the reduction of comprehensive cost by adding chargers to the solution of the first sub-problem, is proved to be an unconstrained submodular set function maximization problem, and can be solved by a 1/2-approximation randomized linear time algorithm for its equivalent problem. Through extensive simulations, we demonstrate that the proposed solution can reduce the comprehensive cost by 57.55% comparing with the benchmark algorithms.

CCS Concepts: • **Networks** → *Network control algorithms*; • **Theory of computation** → *Scheduling algorithms*.

Additional Key Words and Phrases: multi-hop wireless charging, magnetic resonance, charger deployment, submodular function

ACM Reference Format:
Sixu Wu, Lijie Xu, Haipeng Dai, Linfeng Liu, Fu Xiao, and Jia Xu. 2022. Optimizing Comprehensive Cost of Charger Deployment in Multi-hop Wireless Charging. 1, 1 (February 2022), 24 pages. https://doi.org/XXXXXXX.XXXXXXX

1 INTRODUCTION

Wireless Rechargeable Sensor Network (WRSN) has witnessed huge development and attracted more and more attentions from both academic and industrial circles in recent years. There are many applications based on WRSN in various fields, such as automobile, military target tracking and surveillance, natural disaster relief, biomedical health monitoring, and hazardous environment exploration [17]. The cost and efficiency of power transform of WRSN largely depends on the

*Corresponding author

Authors' addresses: Sixu Wu, 2021070711@njupt.edu.cn; Lijie Xu, ljxu@njupt.edu.cn, Jiangsu Key Laboratory of Big Data Security and Intelligent Processing, Nanjing University of Posts and Telecommunications, 9 Wenyuan Rd, Nanjing, Jiangsu, China; Haipeng Dai, haipengdai@nju.edu.cn, The State Key Laboratory for Novel Software Technology, Nanjing University, 163 Xianlin Avenue, Nanjing, Jiangsu, China; Linfeng Liu, liulf@njupt.edu.cn; Fu Xiao, xiaof@njupt.edu.cn; Jia Xu, xujia@njupt.edu.cn, Jiangsu Key Laboratory of Big Data Security and Intelligent Processing, Nanjing University of Posts and Telecommunications, 9 Wenyuan Rd, Nanjing, Jiangsu, China.

wireless charging technology. Different technologies, such as magnetic resonance [19, 25], inductive coupling [9, 22], RF [4, 26, 31, 34] and microwave [7], have different properties and are applicable for various scenarios.

Magnetic resonance wireless charging technology can be easily realized by using copper coils with low cost. More importantly, magnetic resonance has higher charging efficiency than low power charging such as RF. As shown in [25], through physical experiments with distance of $1m$, the charging efficiency of magnetic resonance is 0.78. However, the charging efficiency of RF is less than 0.01 when the distance is $1m$ [15]. In addition, the charging efficiency of magnetic resonance wireless charging depends on the receiver and transmitter's circuitry characteristics and the distance between the two devices [21]. The energy can be transmitted without the source and capture device sitting next to each other or being perfectly aligned [30]. Therefore, the direction of copper coils will not affect the charging efficiency. In principle, the physical properties of coils determine the charging efficiency of magnetic resonance wireless charging. Better charging efficiency can be obtained by increasing the radii of the coils. Therefore, compared with low power charging, magnetic resonance is more suitable for multi-hop wireless charging, and can still maintain considerable charging efficiency after several hops.

From the view of whether the energy can be relayed, wireless charging technology can be classified as multi-hop wireless charging [25, 27, 35] and single-hop wireless charging [4, 8, 26, 33, 34]. In the traditional single-hop wireless charging, the sensor nodes only receive energy from the chargers. However, in the multi-hop wireless charging, the sensor nodes can receive energy from both the chargers and other sensor nodes. This means that the sensor nodes have the function of charging other sensor nodes in multi-hop wireless charging.

The multi-hop wireless charging has promising advantages comparing with the single-hop wireless charging: (1) Multi-hop wireless charging can be viewed as a flexible extension of single-hop wireless charging. As illustrated in Fig. 1, the charging efficiency from sensor node 1 to sensor node 3 is 0.6 if the energy is transferred directly. If the energy is transferred via sensor node 2, the charging efficiency is 0.9*0.9=0.81. Thus, the charging efficiency increases through multi-hop wireless charging. On the other hand, in the multi-hop wireless charging setting, we can still choose the single-hop path if the charging efficiency of single-hop path is better than that of multi-hop path. In fact, multi-hop wireless charging integrates the advantages of single-hop path and multi-hop path, thus, the charging efficiency can be further optimized. (2) In some specific scenarios, single-hop wireless charging is not applicable. For example, in building structure monitoring or disaster relief, the chargers cannot be placed in desirable posotions due to environmental constraints. The energy can only be indirectly transferred to the target sensor nodes in the way of multi-hop relay. (3) The moving cost of mobile chargers can be reduced through multi-hop wireless charging since the number of charging positions decreases. (4) Because the sensor nodes can relay the energy through multi-hop wireless charging, the mobile chargers only need to visit a few sensor nodes in mobile charging, therefore, the moving cost or the number of mobile chargers can be reduced.

As a practical project, WiTricity [30] designed a multi-hop wireless charging application based on magnetic resonance. The resonant repeaters are placed between the source and receiver to extend the wireless charging range. The energy can be transferred to greater distances through multi-hop relays. Additionally, there are theoretical studies on multi-hop wireless charging [21, 25, 32]. However, they aimed to optimize the single objective, such as minimizing the number of chargers, moving cost, or energy consumption. For example, Wang *et al.* [25] optimized the energy cost of multi-hop wireless charging in mobile charging scenario. Rault *et al.* [21] aimed to find the least chargers that can fulfill the energy demands of all sensor nodes. However, considering the single objective cannot accurately represent the actual cost in complex real-world scenarios.

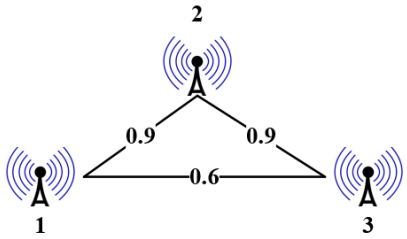

Fig. 1. Illustration of multi-hop wireless charging. The numbers on the edges represent the charging efficiency.

In this paper, we consider the actual comprehensive cost of wireless charging consisting of energy cost and deployment cost. The energy cost is the expenditure for energy consumption (e.g., the payment to energy provider). The deployment cost is the expenditure for deploying wireless chargers (e.g., rental fee, depreciation allowances, or installation cost). In general, deployment cost is related to the number of wireless chargers. We aim to optimize the comprehensive cost, which is the summation of energy cost and deployment cost, such that the energy demand of all sensor nodes can be fulfilled by energy capacitated chargers in the way of multi-hop energy transfer. Because the energy forwarding of every hop will lead to energy loss, the energy loss increases accordingly with the increasing number of hops. It is possible to reduce the overall energy consumption by deploying more chargers, but this will increase the deployment cost.

There are three modes of multi-hop wireless charging technology: store and forward, direct flow, and hybrid [27]. In store and forward mode, each sensor node accepts and stores energy first, and then forwards it to the sensor nodes of next hop. In the direct flow mode, the energy is directly sent to the target node via multiple hops. The hybrid mode is a mixture of the above two modes. This work is based on the store and forward mode.

Since the multi-hop wireless charging in this paper is based on magnetic resonance technology, a special problem of magnetic resonance called "conflict" has to be taken into account [25]. If multiple transmitters charge the same receiver simultaneously, the magnetic fields of the transmitters will affect each other. If they are not exactly in the same direction, there will be partial offset, resulting in energy loss. In order to reduce unnecessary losses, we need to avoid the occurrence of "conflict". In theory, we can avoid "conflict" through clock synchronization, of which the accuracy is largely related to the synchronization time interval. In most clock synchronization algorithms, the synchronization time interval is dozens of seconds [6, 11]. Therefore, the communication overhead increases significantly due to the periodic clock synchronization message propagation. Moreover, clock synchronization will take more time to finish the charging due to the time-division. Therefore, we aim to avoid "many-to-one" charging when we optimize the comprehensive cost. Note that "one-to-many" charging is feasible.

The problem of optimizing the comprehensive cost for charger deployment in multi-hop wireless charging in WRSN is very challenging. Our problem is a variation of *Facility Location Problem (FLP)* [1]. We can consider the chargers and the sensor nodes as the facilities and the clients, respectively. However, the main difference between our problem and *FLP* is that we need to ensure all sensor nodes along the same energy flow are charged by the same charger in order to avoid "conflict". The energy flow means that energy will flow to the sensor nodes via multiple hops. The common solutions [1] of *FLP* are invalid for our problem because any client can be connected to any facility in *FLP*.

The main contributions of this paper are as follows:

- We present a novel multi-hop wireless charging model and formulate the *Capacitated Minimum Charging Forest* (*CMCF*) problem, which is proved to be NP-hard.
- We decompose the *CMCF* problem into two sub-problems, and present a two-stage solution to optimize the comprehensive cost. We propose a greedy algorithm for the first sub-problem, and solve the second sub-problem through a (1/2)-approximation algorithm for its equivalent problem.
- Through extensive simulations, we demonstrate that the proposed solution shows significant superiority in terms of comprehensive cost. Moreover, the proposed solution shows strong adaptivity for parameter variations.

The rest of the paper is organized as follows. Section 2 presents a brief review on the previous works. Section 3 presents the system model and problem formulation. Section 4 presents the details of our solution. Performance evaluation is shown in Section 5. In Section 6, we discuss two important problems in actual charging. We conclude this paper in Section 7.

2 RELATED WORK

In this section, we briefly review the related studies on single-hop wireless charging and multi-hop wireless charging.

2.1 Single-hop Wireless Charging

As the traditional charging mode, single-hop wireless charging has been widely studied. Dai *et al.* [4] studied the problem of charging task scheduling for directional wireless charger networks. They scheduled the orientations of chargers with time in centralized offline and distributed online fashions to maximize the overall charging utility for all tasks. In [13], Lin *et al.* explored the wireless signal propagation process and provided a theoretical charging model to enhance charging efficiency by leveraging obstacles. Utilizing the concept of the *Fresnel Zones*, they reformalized the wireless charging model and discretized charging power to determine the best charging spots as well as charging durations, which can maximize the charging efficiency. In [15], the authors proposed a pragmatic energy transfer model verified by experiments. They proposed a problem to reduce charging delay in directional wireless charging and formulated the problem as a linear programming problem. The proposed method achieved the goal of reducing the charging delay and could reduce the charging energy, which is not completely equivalent to the optimization of actual cost. Lin *et al.* [14] addressed the issue of how to serve the 3-D WRSN with an unmanned aerial vehicle (UAV). The objective is to maximize the charged energy for sensors supplied by the UAV with energy constraint. However, the scenario for UAV was very different from that of this paper. In [16], the authors aimed to jointly optimize the number of dead sensors and the energy usage effectiveness in the multi-node charging scenarios, and proposed a multi-node temporal spatial partial-charging algorithm (MTSPC) to solve it. In [23], Tomar *et al.* proposed a novel charging scheme, which integrated two popular multi-attribute decision making methods, to determine charging schedule by evaluating various network attributes, namely residual energy, distance to mobile charger, energy consumption rate, and neighborhood energy weightage. The studies mentioned above had various goals, but they did not consider the cost or only taked the cost as a constraint. In this paper, we aim to minimize the cost, which is a practical concern in the vast majority of WRSN.

[20] proposed a multi-node charging vehicle scheduling scheme following a partial charging model to minimize the energy spent on traveling and maximize the network lifetime. First, the charging schedules of multiple charging vehicles were generated through optimal halting points by integrating non-dominated sorting genetic algorithm and multi-attribute decision making approach. Then the charging time at each halting point was decided for the sensor

nodes with the help of a partial charging timer. In order to reduce the moving cost of mobile charger, [36] relaxed the strictness of perpetual operation by allowing some sensor nodes to temporarily run out of energy while still maintaining target k-coverage in a network. In our paper, the charging demands of all sensor nodes should be fully satisfied. In [26], the authors aimed to find the optimal trajectory planning for a mobile charger in terms of energy minimization. They first found the initial charging clusters and the charging path, and then improved the path to reduce energy consumption. However, in their paper, the multi-hop wireless charging was not involved.

2.2 Multi-hop Wireless Charging

The physical properties of multi-hop wireless charging technology for WRSNs has been studied extensively [10, 28, 35]. However, these papers did not consider the optimization problems based on multi-hop wireless charging.

There are some researches on multi-hop wireless charging in WRSN. Rault *et al.* [21] aimed to place the chargers on sensor nodes and proposed an optimization model of minimizing the number of chargers, which transferred energy to sensor nodes in the multi-hop wireless charging scenario. However, they did not take into consideration the energy consumption. Wu *et al.* [32] proposed the repeater deployment method to realize full multi-hop wireless charging coverage of WRSN such that the number of resonant repeaters is minimized. They designed the rules to remove redundant repeaters and optimized the positions of necessary repeaters to improve the charging efficiency. The system model of [32] is very different from this paper since there is no need to deploy additional repeaters in our charging system.

In [25] and [12], the researchers considered the multi-hop wireless charging in the mobile charging scenario. With the multi-hop wireless charging technology, it is not necessary to visit all sensor nodes in the network. Wang *et al.* [25] carried out the regional partition through set cover algorithm, and then designed an algorithm to schedule the mobile chargers. They set a efficiency threshold to determine the candidate charging sets and then select some candidate charging sets to cover all sensor nodes. For each sensor node, its candidate charging set is composed of the nearby sensor nodes, of which the charging efficiencies are larger than the efficiency threshold. However, the efficiency threshold, which largely influence the energy consumption of mobile chargers, is hard to be predetermined. Li *et al.* [12] proposed an energy efficient mobile multi-hop wireless charging strategy. By introducing the optimal central point-based polling point selection algorithm, they constructed the best arrest point of each partition for the mobile charger. In each partition, the multi-hop wireless charging was adopted to replenish energy for these nodes. These studies also did not optimize the energy consumption and deployment cost jointly. In this paper, we aim to optimize the total comprehensive cost, which is the actual expenditure to obtain wireless charging service.

Table 1 shows the difference between our paper and related works in terms of optimization problems.

3 SYSTEM MODEL AND PROBLEM FORMULATION

In this section, we present the system model and formulate the problem. We list the frequently used notations in Table 2.

3.1 System Model

We consider that there is a wireless rechargeable sensor network consisting of a set V of n sensor nodes. All sensor nodes have the ability of energy store and energy forward. Each sensor node $j \in V$ has an energy demand $D_j \geq 0$. We denote the energy demand profile of all sensor nodes as $\mathbf{D} = (D_1, D_2, ..., D_n)$. In this paper, we consider the case where it is impossible to set up additional chargers. The chargers are deployed at the positions of sensor nodes since

Table 1. Summary of optimization problems in related works.

Paper	Satisfy full demands of all sensor nodes	Optimize deployment cost	Optimize energy consumption	Use multi-hop wireless charging technology
[4][13][14][16][23]	No	No	No	No
[15]	Yes	No	No	No
[20][36]	No	No	Yes	No
[26]	Yes	No	Yes	No
[21]	Yes	Yes	No	Yes
[32]	Yes	No	No	Yes
[25][12]	Yes	No	Yes	Yes
Our paper	Yes	Yes	Yes	Yes

Table 2. Frequently Used Notations

Symbol	**Description**
$V,\ n$	Set of sensor nodes, number of sensor nodes
D_j	Energy demand of sensor node j
r	Maximum charging range of sensor node
π_{ij}	Loss coefficient from i to j
$D_{\mathrm{MAX}},\ D_r$	Energy capacity of charger, residual energy of charger
$\alpha,\ \beta$	Unit energy cost, unit deployment cost
$G(V,E)$	Charging network
$\mathcal{T},\ T_i$	Charging forest, charging tree with root i
$V_i,\ E_i$	Set of sensor nodes in T_i, set of edges in T_i
P_{ij}	Path from i to j
$E_{P_{ij}},\ V_{P_{ij}}$	Set of edges in path P_{ij}, set of sensor nodes in path P_{ij}
V_u	Set of uncovered sensor nodes
C_1	Set of charger positions of stage 1
$\Delta F(\cdot)$	Function of comprehensive cost reduction

the charger deployment can be viewed as making workers move to the positions of sensor nodes for charging. The sensor nodes receiving energy from workers directly can be viewed as the chargers in the network. We reuse V as the set of candidate positions for charger deployment.

We consider that the sensor nodes are homogeneous and have identical energy capacity D_{MAX}, $D_{\mathrm{MAX}} \gg D_j$, for all $j \in V$. When a task of direct charging is completed, the worker who completes the task is paid β, which is the deployment cost.

Each sensor node can transfer energy to other nodes within the maximum charging range r as energy repeaters through magnetic resonance wireless charging technology if its energy demand is satisfied. We consider that the sensor nodes have the same maximal charging range. We denote by $\pi_{ab} \geq 1$ the loss coefficient between any two sensor nodes $a, b \in V$ within the maximal charging range. In other words, if the energy demand of b is D_b, a needs to transfer energy of $\pi_{ab} D_b$ to b. The loss coefficient depends on the circuitry design of magnetic resonance and the distance between the two sensor nodes [19], and will be formulated and calculated in simulation setup (Section 5.1). According to [21], the charging efficiency is symmetrical, i.e., $\pi_{ab} = \pi_{ba}$ for any two sensor nodes $a, b \in V$.

Since a worker charges a sensor node directly in a very small distance, the sensor node can be charged with negligible energy loss, i.e., $\pi_{ab} = 1$ iff $a = b$. Then the sensor node transfers the stored energy in excess of the demand to other adjacent sensor nodes with energy loss.

We define the charging network as follows:

Definition 1 (Charging Network). *The charging network is an undigraph $G(V, E)$, where V is the set of sensor nodes, E is the set of edges connecting the sensor nodes with distance less than the maximal charging range. Each edge $(a, b) \in E$ is with a loss coefficient $\pi_{ab} \geq 1$.*

Although there is energy loss in battery energy storage in store and forward based multi-hop wireless charging due to the self discharge, the self discharge rate of lithium-ion battery is 2%-3% per month [3]. The time of storage process in multi-hop wireless charging is rather short, and the storage loss can be neglected.

For any two sensor nodes $i, j \in V$, $(i, j) \notin E$, the initial loss coefficient between i and j is infinite. However, if j obtains energy from i via a path P_{ij} on $G(V, E)$, the loss coefficient between i and j can be calculated as:

$$\pi_{ij} = \prod_{(a,b)\in E_{P_{ij}}} \pi_{ab} \tag{1}$$

where $E_{P_{ij}}$ is the set of edges in path P_{ij}.

Note that a sensor node cannot be charged by multiple chargers simultaneously due to the conflict of magnetic resonance wireless charging. Thus, if sensor node j is charged via path P_{ij} by charger i, all sensor nodes in the path must be charged by charger i too. In order to satisfy the energy demand of all nodes in path P_{ij}, the energy of charger i should be at least $\sum_{j'\in V_{P_{ij}}} \pi_{ij'} D_{j'}$, where $V_{P_{ij}}$ is the set of sensor nodes in path P_{ij}. Any charger i can charge multiple sensor nodes via different paths. The paths with same source i together construct a charging tree.

Definition 2 (Charging Tree). *The charging tree is a subgraph of charging network $G(V, E)$. The charger locates in the root of charging tree, and the sensor nodes in charging tree (including the sensor node located in the root) are charged by the charger via the path of charging tree.*

We denote the charging tree with root $i \in V$ as T_i. The energy cost of charging tree T_i is $\alpha \sum_{j\in V_i} \pi_{ij} D_j$, where α is the unit energy cost and V_i is the set of sensor nodes in T_i. Since a sensor node cannot be charged by multiple chargers, the deployment of chargers will divide the charging network into multiple disjoint charging trees, which construct a charging forest.

Definition 3 (Charging Forest). *The charging forest $\mathcal{T} = \{T_1, T_2, \ldots, T_n\}$ is a partition of charging network $G(V, E)$ by the disjoint charging trees.*

We use an example in Fig. 2 to illustrate the charging tree, charging forest, and energy cost of charging tree. There are 3 disjoint charging trees in the charging forest. Specifically, there are 7 sensor nodes in the right charging tree. The combination of charger and sensor node 1 is represented by the rectangle. The sensor nodes are represented by the disks. The number beside the sensor node represents its energy demand, and the number on the edge represents its loss coefficient, i.e., $D_1 = D_5 = 2$, $D_2 = D_6 = 3$, $D_3 = D_4 = 4$, $D_7 = 5$, $\pi_{11} = 1$, $\pi_{12} = 1.1$, $\pi_{14} = \pi_{17} = \pi_{23} = 1.2$, $\pi_{45} = 1.3$, $\pi_{46} = 1.4$. Based on (1), we have $\pi_{13} = \pi_{12}\pi_{23} = 1.32$, $\pi_{15} = \pi_{14}\pi_{45} = 1.56$, $\pi_{16} = \pi_{14}\pi_{46} = 1.68$. Then, the energy cost of charging tree T_1 is $\alpha \sum_{j\in V_1} \pi_{1j} D_j = 29.54\alpha$.

Definition 4 (Comprehensive Cost). *The comprehensive cost F is the sum of energy cost and deployment cost:*

$$F{=}\alpha \sum_{i\in V} y_i \sum_{j\in V} \pi_{ij} D_j x_{ij} + \beta \sum_{i\in V} y_i \tag{2}$$

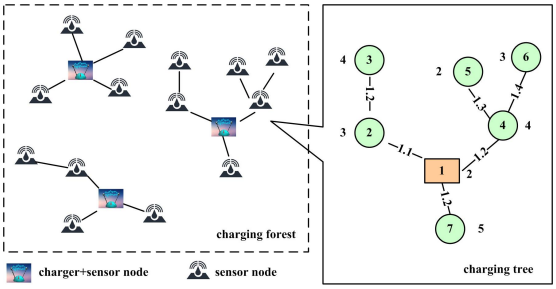

Fig. 2. Illustration of charging tree, charging forest, and energy cost.

where $x_{ij} \in \{0,1\}$ *is the binary variable to indicate whether sensor node* j *is charged by charger* i. $y_i \in \{0,1\}$ *is the binary variable to indicate whether a charger is placed at position* i.

3.2 Problem Formulation

Our objective is to construct the charging forest with capacitated energy of charger by determining x_{ij} and y_i such that the comprehensive cost is minimized. We refer to this problem as *Capacitated Minimum Charging Forest* (*CMCF*) problem, which can be formulated as follows:

$$\min F{=}\alpha \sum_{i\in V} y_i \sum_{j\in V} \pi_{ij} D_j x_{ij} + \beta \sum_{i\in V} y_i \tag{3}$$

$$s.t. \sum_{i\in V} x_{ij} = 1,\ \forall j \in V \tag{3a}$$

$$\sum_{j\in V} \pi_{ij} D_j x_{ij} \le D_{\mathrm{MAX}}\, y_i, \forall i \in V \tag{3b}$$

$$x_{ij'} = 1,\ \forall j' \in V_{P_{ij}},\ y_i = 1,\ x_{ij} = 1 \tag{3c}$$

$$x_{ij} \in \{0,1\},\ \forall i,j \in V \tag{3d}$$

$$y_i \in \{0,1\},\ \forall i \in V \tag{3e}$$

The constraint (3a) ensures that each sensor node is charged by exactly one charger. The constraint (3b) ensures that the energy cost of a charging tree is no more than the energy capacity of the charger. The constraint (3c) guarantees that we can get the disjoint charging trees. In other words, if a sensor node is charged by one charger, then all sensor nodes in the path of charging tree from the charger to the sensor node should be charged by the same charger.

4 ALGORITHM DESIGN FOR *CMCF* PROBLEM

In this section, we present the solution for *CMCF* problem.

4.1 Hardness and Design Rationale

We attempt to find an optimal algorithm for the *CMCF* problem. Unfortunately, as the following theorem shows, the *CMCF* problem is NP-hard.

Theorem 1. *The CMCF problem is NP-hard.*

Proof: We consider the special case of *CMCF* problem by removing the constraint (3c). We demonstrate that the special case of *CMCF* problem belongs to NP firstly. Given an instance of the special case of *CMCF* problem, we can check whether all sensor nodes are covered and check whether the comprehensive cost is at most v. This process can terminate in polynomial time.

Then, we prove the NP-hardness of the special case of *CMCF* problem by giving a polynomial time reduction from the *Single Source Capacitated Facility Location Problem* (*SSCFLP*) [1], which is a well-known NP-hard problem.

Instance of *SSCFLP* (denoted by A): For a set $V = \{1, 2, \cdots, n\}$ of n positions. Each position has a client and a facility. Each client $j \in V$ has a demand D_j that must be served by one open facility. The cost for serving one-unit demand of client j from facility i is $\alpha\pi_{ij}$. Let β represent the cost of opening any facility $i \in V$. Let D_{MAX} represent the maximum demand that facility can serve. The question is to find a subset of open facilities such that the demand of each client is met by an open facility and the total cost of facility opening and client service is at most v.

We consider a corresponding instance of the special case of *CMCF* problem (denoted by B): For a set $V = \{1, 2, \cdots, n\}$ of n positions. Each position has a sensor node. The candidate positions for charger deployment are V. Each sensor node $j \in V$ has an energy demand D_j that must be charged by one charger. Let α represent the unit energy cost. Let π_{ij} represent the loss coefficient for charging sensor node j from charger i. Therefore, the cost for charging one-unit energy of sensor node j from charger i is $\alpha\pi_{ij}$. Let β represent the deployment cost of any charger $i \in V$. Let D_{MAX} represent the energy capacity that charger can serve. The question is to find a subset of positions for charger deployment such that the energy demand of each sensor node is met by a charger and the total cost of charger deployment and energy cost is at most v.

This reduction from A to B ends in polynomial time. We can simply see that q is a solution to A if and only if q is a solution to B. ■

Since the *CMCF* problem is NP-hard, it is impossible to obtain the optimal solution in polynomial time unless P=NP. In addition, we cannot use the off-the-shelf algorithms [1, 24] for *SSCFLP* since we need to guarantee that the solution produces the disjoint charging trees.

The design rationale of our solution is to decompose the *CMCF* problem into two sub-problems. The first sub-problem aims to minimize the deployment cost while satisfying all the constraints of *CMCF* problem given in (3). Then the second sub-problem aims to reduce the comprehensive cost based on the outcome of the first sub-problem. The whole process consists of the following two stages:

Stage 1: Charging Forest Initialization

In this stage, we aim to initialize a charging forest to cover all sensor nodes such that the total deployment cost is minimized. Since the deployment cost of each charger is fixed, this problem is equivalent to minimizing the number of chargers. Specifically, we construct a charging tree for each unselected position with maximum sensor nodes by construction of *Minimum Spanning Tree* with capacity constraint. Then we add the charging tree with maximum sensor nodes into the charging forest. The above process follows the greedy approach.

Stage 2: Comprehensive Cost Reduction

In this stage, we add chargers to the charging forest obtained by Stage 1 to reduce the comprehensive cost further. Specifically, we need to find a subset of positions, where the chargers are placed, to maximize the reduction of comprehensive cost. We show that this problem is an unconstrained submodular function maximization problem. Then the $(1/2)$-approximation algorithm can be applied to the equivalent problem [2].

4.2 Charging Forest Initialization

In this section, we initialize a charging forest to cover all sensor nodes such that the number of chargers is minimized. In other words, we aim to use the fewest chargers to cover all sensor nodes while satisfying all the constraints of *CMCF* problem. We refer to this problem as *Capacitated Deployment Cost Optimization* (*CDCO*) problem, which can be formulated as follows:

$$\begin{aligned} &\min \sum_{i \in V} y_i \\ &s.t.\ \text{(3a) - (3e)} \end{aligned} \tag{4}$$

Theorem 2. *The CDCO problem is NP-hard.*

Proof: We demonstrate that *CDCO* belongs to NP firstly. Given an instance of *CDCO*, we can check whether all sensor nodes are covered and check whether the number of chargers is at most v. This process can terminate in polynomial time.

Next, we show the *CDCO* problem is harder than the well-known *Set Cover* (*SC*) problem [5].

Instance of *SC* (denoted by *A*): For a universe set $V = \{1, 2, \cdots, n\}$ of n elements, a family of sets $S = \{S_1, S_2, ..., S_n\}$ and a positive real v. The question is to find a set $S' \subseteq S$ with size at most v such that every element in V belongs to at least one member in S'.

We consider a corresponding instance of *CDCO* (denoted by *B*): For a universe set $V = \{1, 2, \cdots, n\}$ of n sensor nodes and a family of charging tree sets $\mathcal{T} = \{T_1, T_2, ..., T_n\}$. The question is to find a set $\mathcal{T}' \subseteq \mathcal{T}$ with size at most v such that every sensor node in V is assigned to at least one charging tree in $\mathcal{T}'$.

Since the charging tree can be any subset of all uncovered sensor nodes, the number of the charging trees is exponential in *CDCO* problem. Moreover, each charging tree is subject to the energy capacity of the charger. Therefore, the *CDCO* problem is harder than the *Set Cover* problem. ■

Since the *CDCO* problem is NP-hard, it is impossible to compute the optimal solution in polynomial time unless P=NP. We propose an algorithm for the *CDCO* problem based on the well-known greedy algorithm, which is $(\ln n + 1)$-approximation for the *SC* problem [5]. The greedy algorithm iteratively selects a set maximizing the number of newly covered elements. Similarly, for our *CDCO* problem, we iteratively select a charging tree maximizing the number of newly covered sensor nodes with the constraint of energy capacity. We call such charging tree as *Capacitated Maximum Charging Tree* (*CMCT*).

However, the charging tree can be any subset of all uncovered sensor nodes, thus the number of the charging trees is exponential. We cannot find *CMCT* by simple enumeration. To address this problem, we use a modified Prim algorithm to find the *Capacitated Minimum Spanning Tree* (*CMST*) in polynomial time.

Let $T_i = (V_i, E_i)$ be the charging tree with charger i, where V_i and E_i are the sets of sensor nodes and edges in T_i, respectively. Let V_u be the set of uncovered sensor nodes. As illustrated in Algorithm 1, we find *CMST* T_i' for all $i \in V_u$ in each iteration by calling function *CMST*$(\cdot)$ (Line 6). Then we find the *CMST* T_i with maximum size (Line 8). If there are multiple *CMST*s, any one of them can be selected. The iteration terminates when all sensor nodes are covered by the selected *CMST*s.

Note that if the charging forest $\mathcal{T}$ exists, $\mathcal{T}$ must be a partition of $G(V, E)$, i.e., each sensor node in V is covered exactly by one charging tree because of the monotonicity of comprehensive cost F given in (2). Thus, we only construct *CMST* based on the uncovered sensor node set V_u.

Algorithm 1 Charging Forest Initialization

Input: charging network $G(V, E)$, energy capacity D_{MAX}, energy demand profile $\mathbf{D}$
Output: charging forest $\mathcal{T}$
1: **foreach** $i \in V$ **do**
2: $T_i = (V_i, E_i) \leftarrow (\emptyset, \emptyset)$; $V_u \leftarrow V$; $\mathcal{T} \leftarrow \{T_1, T_2, \ldots, T_n\}$;
3: **end**
4: **while** $V_u \neq \emptyset$ **do**
5: **foreach** $i \in V_u$ **do**
6: $T_i' \leftarrow CMST(i, V_u, G(V, E), D_{\text{MAX}}, \mathbf{D})$;
7: **end**
8: $i \leftarrow \arg\max_{i' \in V_u} |V_{i'}'|$;
9: $T_i \leftarrow T_i'$; $V_u \leftarrow V_u \backslash V_i$;
10: **end**
11: **return** $\mathcal{T}$;

As illustrated in Algorithm 2, we use a modified Prim algorithm to find the *CMST*. First, we add the sensor node at position i into the charging tree T_i (Lines 2-4). Then we iteratively add the sensor node outside the charging tree with minimum energy cost into the charging tree. The iteration terminates when the residual energy of charger i is smaller than the energy cost of any sensor node outside the charging tree. Specifically, in each iteration, we find an edge $(j_i, j_o) \in E$ satisfying that j_i is a sensor node in T_i and j_o is a sensor node outside the T_i with minimum $\pi_{ij_i}\pi_{j_ij_o}D_{j_o}$, where $\pi_{ij_i}\pi_{j_ij_o} = \pi_{ij_o}$ is the loss coefficient from charger i to sensor node j_o (Line 8). Then we add the edge (j_i, j_o) and the corresponding sensor node j_o into the charging tree (Lines 10-11).

Algorithm 2 CMST$(\cdot)$

Input: charging network $G(V, E)$, energy capacity D_{MAX}, energy demand profile $\mathbf{D}$, charger i, uncovered sensor nodes V_u
Output: capacitated minimum spanning tree T_i
1: $T_i = (V_i, E_i) \leftarrow (\emptyset, \emptyset)$; $D_r \leftarrow D_{\text{MAX}}$;
2: **if** $D_r - D_i \geq 0$ **then**
3: $V_i \leftarrow V_i \cup \{i\}$; $V_u \leftarrow V_u \backslash \{i\}$; $D_r \leftarrow D_r - D_i$;
4: **else**
5: **return** T_i;
6: **end**
7: **while** $D_r > 0$ **do**
8: $(j_i, j_o) \leftarrow \arg \min_{(j,j') \in E: j \in V_i, j' \in V_u \backslash V_i} \pi_{ij}\pi_{jj'}D_{j'}$;
9: **if** $D_r - \pi_{ij_i}\pi_{j_ij_o}D_{j_o} \geq 0$ **then**
10: $D_r \leftarrow D_r - \pi_{ij_i}\pi_{j_ij_o}D_{j_o}$; $\pi_{ij_o} \leftarrow \pi_{ij_i}\pi_{j_ij_o}$;
11: $V_i \leftarrow V_i \cup \{j_o\}$; $V_u \leftarrow V_u \backslash \{j_o\}$; $E_i \leftarrow E_i \cup (j_i, j_o)$;
12: **else**
13: **return** T_i;
14: **end**
15: **end**

Theorem 3. *The running time of Charging Forest Initialization is* $O(n^5)$.

Proof: Algorithm 2 is dominated by while loop (Lines 7-15), which takes $O(n^3)$ time, where finding the edge with minimum energy cost (Line 8) takes $O(n^2)$. Algorithm 1 is dominated by constructing *CMST* (Line 6), which is executed at most $O(n^2)$ times. Thus, the running time of whole *Charging Forest Initialization* is $O(n^5)$. ■

Remark: The running time of *Charging Forest Initialization*, $O(n^5)$, is very conservative since both the number of charging trees and the number of sensor nodes in any charging tree are much less than n in practice. Moreover, if we use the improved implementation of Prim algorithm instead of the simplified version given in algorithm 2, the running time of *Charging Forest Initialization* can be improved to $O(n^4)$.

4.3 Comprehensive Cost Reduction

In *Charging Forest Initialization* stage, we aim to minimize the deployment cost of chargers. In this subsection, we present the details of *Comprehensive Cost Reduction* stage, in which we add the chargers to the charging forest of *Charging Forest Initialization* stage so as to maximize the reduction of comprehensive cost.

Given any charging tree T_i, if a charger is added at any position $w \in V_i \backslash \{i\}$, T_i would be divided into two charging trees by removing the edge (w', w) where w' is the parent of w in T_i. Such division may reduce the energy cost as the loss coefficient of some sensor nodes are reduced. Fig. 3 illustrates the process of charging tree division by adding a charger at position 4. Note that the new charging tree must be the sub-tree of the original charging tree, thus we do not need to consider the energy constraint when we add charger at any position.

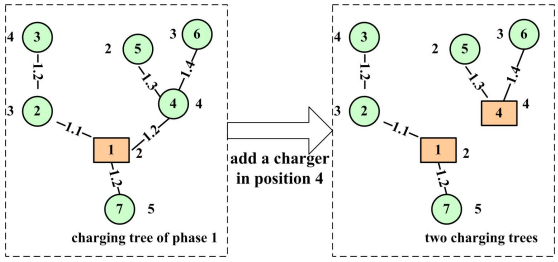

Fig. 3. Illustration of dividing charging tree into two charging trees by adding a charger.

Given the charger position set C_1 of charging forest $\mathcal{T}$ obtained from *Charging Forest Initialization* stage, the objective of *Comprehensive Cost Reduction* is finding a set of positions $C_2 \subseteq V \backslash C_1$ to place the chargers such that the reduction of comprehensive cost is maximized. We refer to this problem as *Comprehensive Cost Reduction Maximization* (*CCRM*) problem, which can be formulated as follows:

$$\max_{C_2} \Delta F(C_2) = -\beta |C_2| + \alpha \Big(\sum_{i \in C_1} \sum_{j \in V_i} \pi_{ij} D_j - \sum_{i \in C_1 \cup C_2} \sum_{j \in V_i'} \pi_{ij} D_j \Big) \tag{5}$$

where $\Delta F(C_2)$ presents the comprehensive cost reduction due to adding chargers at every position of $C_2 \subseteq V \backslash C_1$. $\beta |C_2|$ is the increased deployment cost. $\alpha \big(\sum_{i \in C_1} \sum_{j \in V_i} \pi_{ij} D_j - \sum_{i \in C_1 \cup C_2} \sum_{j \in V_i'} \pi_{ij} D_j \big)$ is the reduction of energy cost through adding chargers at position set C_2. Since there are different charging trees with the same root, we use V_i, V_i', V_i'', and V_i''' to distinguish sensor node sets with the same root but different constituent elements in the same formula.

We give the following definition.

Definition 5 (Submodular Function). *Given a finite ground set V, a real-valued set function defined as $f : 2^V \rightarrow \mathbb{R}$, f is called submodular if $f(A \cup \{w\}) - f(A) \geq f(B \cup \{w\}) - f(B)$ for all $A \subseteq B \subseteq V$ and $w \in V \backslash B$.*

Next, we show that the function $\Delta F(\cdot)$ defined in (5) is a submodular function.

Theorem 4. *The comprehensive cost function $\Delta F(\cdot)$ is a submodular function.*

Proof:

$$\begin{aligned}
&\Delta F(A \cup \{w\}) - \Delta F(A) \\
&= -\beta(|\mathrm{A}| + 1) + \alpha\Big(\sum_{i \in C_1} \sum_{j \in V_i''} \pi_{ij} D_j - \sum_{i \in C_1 \cup A \cup \{w\}} \sum_{j \in V_i'} \pi_{ij} D_j\Big) \\
&\quad - \big(-\beta(|\mathrm{A}|) + \alpha\Big(\sum_{i \in C_1} \sum_{j \in V_i''} \pi_{ij} D_j - \sum_{i \in C_1 \cup A} \sum_{j \in V_i} \pi_{ij} D_j\Big)\big) \\
&= -\beta + \alpha\Big(\sum_{i \in C_1 \cup A} \sum_{j \in V_i} \pi_{ij} D_j - \sum_{i \in C_1 \cup A \cup \{w\}} \sum_{j \in V_i'} \pi_{ij} D_j\Big) \qquad (6)
\end{aligned}$$

Similarly, we have:

$$\Delta F(B \cup \{w\}) - \Delta F(B) = -\beta + \alpha\Big(\sum_{i \in C_1 \cup B} \sum_{j \in V_i} \pi_{ij} D_j - \sum_{i \in C_1 \cup B \cup \{w\}} \sum_{j \in V_i'} \pi_{ij} D_j\Big) \qquad (7)$$

Then, we consider the following two cases according to the position of w:

Case 1: $w \in V_i,\ i \in C_1 \cup A$, i.e., w doesn't locate in the charging trees with roots in $B \backslash A$. We further consider the following two subcases:

Case 1.1: w is not on the path from i to any sensor node in $B \backslash A$. In this case, the same division happens on either $C_1 \cup A$ or $C_1 \cup B$. Due to the fact that the energy cost only changes in T_w, we have:

$$\begin{aligned}
&\sum_{i \in C_1 \cup A} \sum_{j \in V_i} \pi_{ij} D_j - \sum_{i \in C_1 \cup A \cup \{w\}} \sum_{j \in V_i'} \pi_{ij} D_j \\
&= \sum_{j \in V_w} \pi_{ij} D_j - \sum_{j \in V_w} \pi_{wj} D_j \\
&= \sum_{i \in C_1 \cup B} \sum_{j \in V_i''} \pi_{ij} D_j - \sum_{i \in C_1 \cup B \cup \{w\}} \sum_{j \in V_i'''} \pi_{ij} D_j \qquad (8)
\end{aligned}$$

Combining (6), (7), and (8), we have:

$$\Delta F(A \cup \{w\}) - \Delta F(A) = \Delta F(B \cup \{w\}) - \Delta F(B)$$

Case 1.2: w is on the paths from i to any sensor node in $B \backslash A$. We have $\sum_{i \in C_1 \cup B} \sum_{j \in V_i} \pi_{ij} D_j - \sum_{i \in C_1 \cup B \cup \{w\}} \sum_{j \in V_i'} \pi_{ij} D_j = \sum_{j \in V_w'} \pi_{ij} D_j - \sum_{j \in V_w'} \pi_{wj} D_j, V_w' \subset V_w$. Since $V_w' \subset V_w$, by using the similar deduction of Case 1.1, we can obtain:

$$\Delta F(A \cup \{w\}) - \Delta F(A) > \Delta F(B \cup \{w\}) - \Delta F(B)$$

Case 2: $w \in V_i, i \in B \backslash A$, i.e., w locates in the charging trees with roots in $B \backslash A$. Without loss of generality, we consider that T_i is a sub-tree of $T_{i'}$ before division. We have:

$$\sum_{i \in C_1 \cup A} \sum_{j \in V_i} \pi_{ij} D_j - \sum_{i \in C_1 \cup A \cup \{w\}} \sum_{j \in V_i'} \pi_{ij} D_j = \sum_{j \in V_w} \pi_{i'j} D_j - \sum_{j \in V_w} \pi_{wj} D_j \qquad (9)$$

$$\sum_{i \in C_1 \cup B} \sum_{j \in V_i} \pi_{ij} D_j - \sum_{i \in C_1 \cup B \cup \{w\}} \sum_{j \in V_i'} \pi_{ij} D_j = \sum_{j \in V_w} \pi_{ij} D_j - \sum_{j \in V_w} \pi_{wj} D_j \qquad (10)$$

For each $j \in V_w$, since P_{ij} is a sub-path of $P_{i'j}$, we have:

$$\pi_{i'j} > \pi_{ij} \tag{11}$$

Combining (6), (7), (9), (10), and (11), we have:

$$\Delta F(A \cup \{w\}) - \Delta F(A) > \Delta F(B \cup \{w\}) - \Delta F(B)$$

Thus $\Delta F(\cdot)$ is submodular. ■

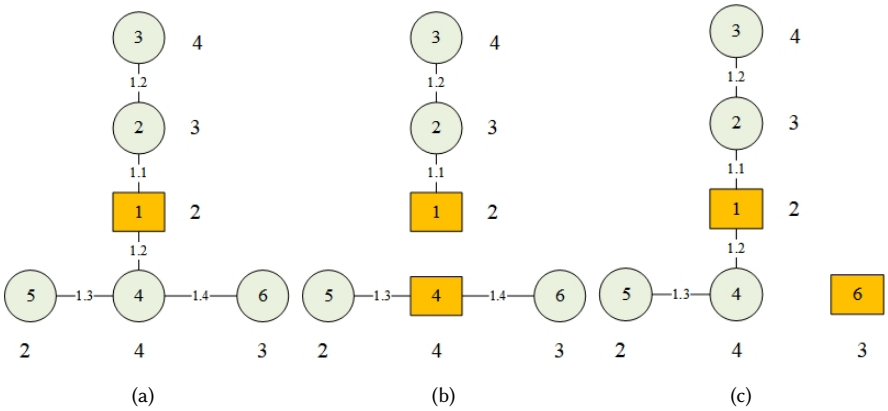

Fig. 4. A simple example to describe the proof process. (a) Charging tree T_1. (b) The case of $B\backslash A = \{4\}$. (c) The case of $B\backslash A = \{6\}$.

We use a simple example given in Fig. 4 to describe the proof process of Theorem 4. The meanings of the numbers in Fig. 4 are same with Fig. 2. According to $C_1 \cup A$ and $C_1 \cup B$, we will have two charging forests. Consider that the only difference of the two charging forests is the charging tree T_1 in Fig. 4(a).

Case 1.1: As shown in Fig. 4(b), let $w = 2$, $B\backslash A = \{4\}$, the energy savings in two cases are the same obviously.

Case 1.2: As shown in Fig. 4(c), Let $w = 4$, $B\backslash A = \{6\}$, we have $V'_w = \{4, 5\}$ and $V_w = \{4, 5, 6\}$. When we add w into $C_1 \cup A$, the energy reduction is (1.2-1)*4+(1.2*1.3-1.3)*2+(1.2*1.4-1.4)*3=2.16. When we add w into $C_1 \cup B$, the energy reduction is (1.2-1)*4+(1.2*1.3-1.3)*2=1.32<2.16.

Case 2: As shown in Fig. 4(b), let $w = 6$, $B\backslash A = \{4\}$. When we add w into $C_1 \cup A$, the energy reduction is (1.2*1.4-1)*3=2.04. When we add w into $C_1 \cup B$, the energy reduction is (1.4-1)*3=1.2<2.04.

Based on Theorem 4, we can conclude that the *CCRM* problem is the problem of submodular set function maximization in the unconstrained setting, which is a well-known NP-hard problem [2]. When the submodular set function is non-negative, it is known that a randomized linear time algorithm provides a $(1/2)$-approximation. Unfortunately, $\Delta F(\cdot)$ can be negative. To circumvent this issue, let $\Delta\mathcal{F}(C_2) = \Delta F(C_2) + \beta n$. It is clear that $\Delta\mathcal{F}(C_2) \geq 0$ for any $C_2 \subseteq V$. Since βn is a constant, $\Delta\mathcal{F}(C_2)$ is also submodular. In addition, maximizing $\Delta F(\cdot)$ is equivalent to maximizing $\Delta\mathcal{F}(\cdot)$.

Therefore, we design the algorithm of *Comprehensive Cost Reduction* based on the algorithm in [2], as illustrated in Algorithm 3. We define two position sets X and Y, where X is empty and Y is the set of all possible positions to add chargers. For each position $w \in V\backslash C_1$, we denote a and b as the non-negative comprehensive cost reduction of including w to X and excluding w from Y, respectively (Lines 3-4). Then we randomly choose whether to include or

Algorithm 3 Comprehensive Cost Reduction

Input: function $\Delta\mathcal{F}(\cdot)$, charging network $G(V, E)$, charging forest $\mathcal{T}$, energy demand profile $\mathbf{D}$, charger set of charging forest C_1, unit energy cost α, unit deployment cost β
Output: charger position set X

```
1: X ← ∅; Y ← V\C_1;
2: foreach w ∈ V\C_1 do
3:   a ← max{ΔF(X ∪ {w}) − ΔF(X), 0};
4:   b ← max{ΔF(Y\{w}) − ΔF(Y), 0};
5:   if a = b then
6:     X ← X ∪ {w};
7:   else
8:     with probability a/(a + b) do X ← X ∪ {w};
9:     with probability b/(a + b) do Y ← Y\{w};
10:  end
11: end
12: return X;
```

exclude w with probability proportional to the ratio between a and b (Lines 8-9). Specifically, if $a = b$, w is added into X definitely.

Since Algorithm 3 is a randomized linear time $(1/2)$-approximation algorithm for the non-negative submodular set function maximization in the unconstrained setting, we can obtain the following theorem straightforwardly.

Theorem 5. *Comprehensive Cost Reduction is a polynomial and* $(1/2)$*-approximation algorithm of the equivalent problem.*

Theorem 6. *Let* X^* *be the optimal solution of the second sub-problem, and* X *be a solution returned by Comprehensive Cost Reduction. We have* $\Delta F(X) \geq 1/2(\Delta F(X^*) - n\beta)$.

Proof: According to the definition of $\Delta\mathcal{F}(\cdot)$, we have:

$$\Delta\mathcal{F}(X) = \Delta F(X) + n\beta \tag{12}$$

$$\Delta\mathcal{F}(X^*) = \Delta F(X^*) + n\beta \tag{13}$$

Because *Comprehensive Cost Reduction* is a 1/2 approximation for the equivalent problem of the second sub-problem, we have:

$$\Delta\mathcal{F}(X) \geq 1/2\Delta F(X^*) \tag{14}$$

By combining (12), (13) and (14), we obtain the theorem. ■

Remark: In each loop, we need to traverse all sensor nodes to get the values of a and b. Such a loop needs to be done n times at most. Therefore, the time complexity of *Comprehensive Cost Reduction* is $O(n^2)$.

5 PERFORMANCE EVALUATION

In this section, we perform simulations to evaluate the performance of our proposed algorithm.

5.1 Simulation Setup

We compare our solution (termed *Comprehensive Optimization* for briefness) with following two benchmark algorithms:

- *CFI* (*Charging Forest Initialization*): *CFI* is the Stage 1 of proposed solution, and the algorithms have been given in Section 4.2. *CFI* adopts the modified Prim algorithm (Algorithm 2) to construct charging trees for every position, and then selects the charging tree with the most sensor nodes greedily until all sensor nodes are covered by the selected charging trees.
- *IAASA* (*Improved AASA*) [25]: We modify the *AASA* in [25] by removing the efficiency threshold and adding the energy capacity constraint such that the algorithm can deal with our system model. *IAASA* adopts the modified Prim algorithm (Algorithm 2) to construct charging trees for every position, and then selects the charging tree with the lowest average comprehensive cost (the ratio of comprehensive cost to the size of charging tree) greedily until all sensor nodes are covered by the selected charging trees.

For the simulations, we distribute sensor nodes in a 20 $m \times 20$ m square area to simulate the dense WRSN environment of precision agriculture. There may be different kinds of sensors in a 400 square meter piece of farmland to accurately detect the condition of the piece of farmland. We set $n = 100$, $r = 2m$, $D_{\mathrm{MAX}} = 150KJ$, $\alpha = 0.5$, $\beta = 2.5$ as the default setting, respectively. In our simulations, one unit of energy is $1KJ$. In addition, the energy demand of each sensor node is randomly selected in $[0.8KJ, 1.2KJ]$. For any sensor nodes $a, b \in V$, the loss coefficient is calculated based on [19]:

$$\pi_{ab} = \begin{cases} 1, & a = b \\ \dfrac{16(d_{ab}/\sqrt{l_a l_b})^6}{Q_a Q_b}, & d_{ab} \le r,\ a \neq b \\ \infty, & d_{ab} > r,\ a \neq b \end{cases} \tag{15}$$

where Q_a and Q_b are the quality factors of two resonators. l_a and l_b are the radii of coils. d_{ab} is the distance between a and b. For our simulations, we set all quality factors as 1000 and all coil radii as $0.1m$, although *Comprehensive Optimization* does not impose the assumption of homogeneous sensor nodes. Moreover, we consider $d_{ab} >> l_a$ and $d_{ab} >> l_b$ to guarantee $\pi_{ab} \ge 1$. According to [19], the conditions for the validity of the model given by equation (15) are $d_{ab} \ge 4.8 l_a$ and $d_{ab} \ge 4.8 l_b$. In our simulations, we divide the square area into grids with side length 0.8 m, and then randomly deploy the sensor nodes on the intersections of the grids to ensure that the distance between any two sensor nodes satisfies that π_{ab} is always greater than or equal to 1.

We will vary the value of the key parameters to explore the impacts on all three algorithms. All simulations are run on a Windows machine with Intel(R) Core(TM) i5-8300H CPU and 8 GB memory. Each measurement is averaged over 100 instances.

5.2 Charger Deployment

We first show the charger deployment for 150 sensor nodes of all three algorithms in 20 $m \times 20$ m square area with default setting. We do not use the default number of sensor nodes. This is because with more sensor nodes, we can clearly observe the differences of three algorithms. Fig. 5(a), Fig. 5(b), and Fig. 5(c) depict the output of *CFI*, *IAASA*, and *Comprehensive Optimization*, respectively. We can see that *CFI*, *IAASA*, and *Comprehensive Optimization* construct 61, 69, and 108 charging trees, respectively. This means *Comprehensive Optimization* adds 47 chargers in the Stage 2 to reduce the Comprehensive cost further.

5.3 Impact of Number of Sensor Nodes

Then we change the number of sensor nodes from 25 to 150, and measure the number of chargers, energy consumption, and comprehensive cost of all three algorithms. We can see from Fig. 6(a) that the number of chargers of all three

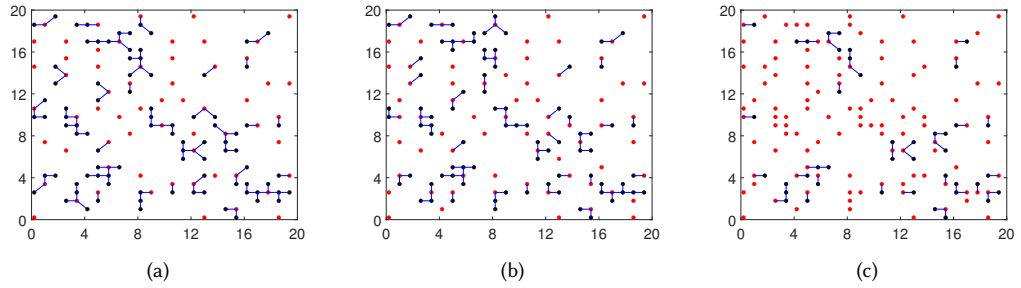

Fig. 5. Charger deployment. The red points represent the positions of chargers. The black points represent the positions without chargers. The sensor nodes of charging trees are connected by blue lines. (a) *CFI*. (b) *IAASA*. (c) *Comprehensive Optimization*.

algorithms increases. This is because the energy demand increases, and the energy capacity is fixed. Therefore, more chargers are needed to satisfy the energy demands of all sensor nodes. The number of chargers of *Comprehensive Optimization* is much more than that of *CFI* and *IAASA* , because *Comprehensive Optimization* tends to reduce the energy consumption by increasing chargers. We can see from Fig. 6(b) that the energy consumption of all algorithms also increases and *Comprehensive Optimization* can obtain the least energy consumption. Although *Comprehensive Optimization* increases 47.73% and 37.58% of the number of chargers on average, comparing with *CFI* and *IAASA*, respectively, our algorithm reduces 73.83% and 55.98% of energy consumption on average, comparing with *CFI* and *IAASA*, respectively.

As shown in Fig. 6(c), *IAASA* reduces 28.59% of comprehensive cost on average, comparing with *CFI*, because *IAASA* selects the charging trees based on the average comprehensive cost. However, *Comprehensive Optimization* always outputs the lowest comprehensive cost, and reduces 44.08% and 21.46% of comprehensive cost on average, comparing with *CFI* and *IAASA*, respectively. In addition, the comprehensive cost of designed algorithm does not increase dramatically with the increase of number of sensor nodes. When there are 150 sensor nodes, the designed algorithm decreases 46.62% and 12.56% of comprehensive cost on average comparing with *CFI* and *IAASA*, respectively. Our algorithm has great scalability in the aspect of comprehensive cost.

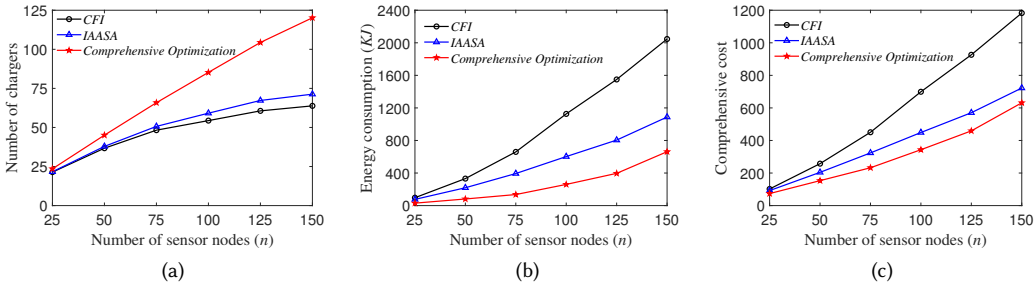

Fig. 6. Impact of number of sensor nodes. (a) Number of chargers. (b) Energy consumption. (c) Comprehensive cost.

5.4 Impact of Energy Capacity of Charger

We increase the energy capacity of charger from 75 to 200, and investigate the impact on three algorithms. As shown in Fig. 7(a), the number of chargers of *CFI* and *IAASA* decreases distinctly. This is because they can construct larger charging trees when the energy capacity increases. However, the number of chargers *Comprehensive Optimization* maintains stable because *Comprehensive Optimization* adds chargers to decrease the comprehensive cost.

We can see from Fig. 7(b) that the energy consumption of *CFI* and *IAASA* increases markedly. When $D_{MAX} = 200KJ$, the energy consumption of *CFI* and *IAASA* increases by 86.03% and 54.15% respectively, comparing with the energy consumption when $D_{MAX} = 75KJ$. This is because the decrease of chargers increases the energy loss. However, *Comprehensive Optimization* can maintain stable energy consumption and reduce 76.05% and 55.68% of energy consumption on average comparing with *CFI* and *IAASA*, respectively.

We can see from Fig. 7(c) that the comprehensive cost of *CFI* and *IAASA* increases markedly. As a contrast, the comprehensive cost of *Comprehensive Optimization* increases rather slowly. *Comprehensive Optimization* always obtains the lowest comprehensive cost, and reduces 48.93% and 23.35% of comprehensive cost on average, comparing with *CFI* and *IAASA*, respectively.

Overall, *CFI* and *IAASA* is sensitive to energy capacity of charger, however, *Comprehensive Optimization* is insensitive to the change of energy capacity. This verifies the strong adaptivity of designed algorithm to various real scenarios.

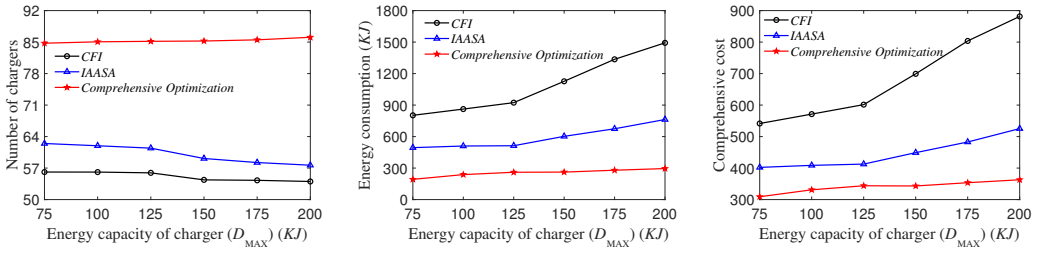

Fig. 7. Impact of energy capacity of charger. (a) Number of chargers. (b) Energy consumption. (c) Comprehensive cost.

5.5 Impact of Energy Demand of Sensor Node

We increase the energy demand of sensor node from $[0.4, 0.8]$ to $[2.4, 2.8]$, and investigate the impact on three algorithms. As shown in Fig. 8(a), the number of chargers of three algorithms increases since more energy is needed. However, in Fig. 8(b), the energy consumption of *CFI* decreases at the beginning and then increases. This is because when the energy demand is large, a charging tree can only cover a few sensor nodes, and the energy loss in transmission becomes smaller. However, even if the number of sensor nodes in the charging tree reduces, the total energy consumption will still increase when the energy demand of each sensor node further increases. Accordingly, the comprehensive cost of *CFI* in Fig. 8(c) shows same trend. We can see from Fig. 8(c), on average, *Comprehensive Optimization* reduces 57.55% and 34.43% of comprehensive cost, comparing with *CFI* and *IAASA*, respectively.

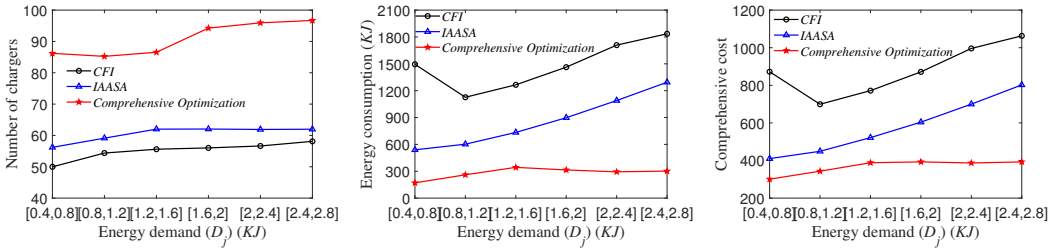

Fig. 8. Impact of energy demand of sensor node. (a) Number of chargers. (b) Energy consumption. (c) Comprehensive cost.

5.6 Impact of Unit Energy Cost

Moreover, we change the unit energy cost from 0.2 to 1.2 to simulate the possible market price relation between energy consumption and charger deployment. We can see from Fig. 9(a) and Fig. 9 (b) that the change of unit energy cost does not impact *CFI* and *IAASA*, which means that the benchmark algorithms are insensitive to the market change. The slight changes of the benchmark algorithms are caused by the random parameters. Different from *CFI* and *IAASA*, our algorithm can deploy more chargers to reduce the energy consumption when the unit energy cost is high, thus the number of chargers of our algorithm increases. When $\alpha = 1.2$, our algorithm increases the number of chargers by 11.99% and reduces the energy consumption by 16.53% comparing with when $\alpha = 0.2$.

We can see from Fig. 9(c) that the comprehensive cost of both *CFI* and *IAASA* increases significantly since the energy consumption of them does not change and unit energy cost increases linearly. On average, our algorithm reduces 51.37% and 25.73% of comprehensive cost, comparing with *CFI* and *IAASA*, respectively.

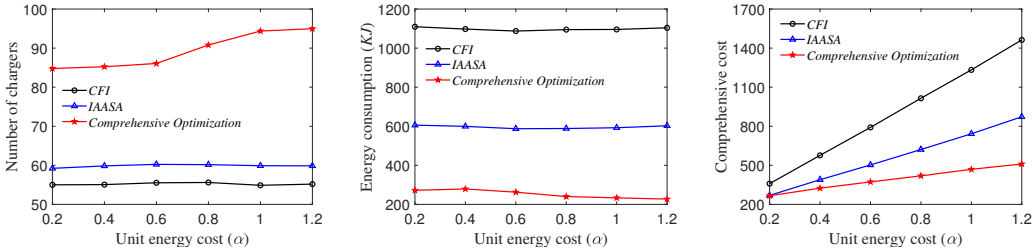

Fig. 9. Impact of unit energy cost. (a) Number of chargers. (b) Energy consumption. (c) Comprehensive cost.

5.7 Impact of Unit Deployment Cost

We also change the unit deployment cost from 1 to 3.5. As shown in Fig. 10(a) and Fig. 10(b), the benchmark algorithms are still insensitive to the market change. However, for our algorithm, the number of chargers when $\beta = 3.5$ decreases by 10.18% comparing with the number of chargers when $\beta = 1$. And the energy consumption when $\beta = 3.5$ increases by 37.13% comparing with the energy consumption when $\beta = 1$. This is because our algorithm tries to mitigate the

increase in comprehensive cost by reducing the number of chargers, which will inevitably lead to the increase in energy consumption. We can see from Fig. 10(c) that, on average, our algorithm reduces 52.46% and 27.03% of comprehensive cost, comparing with *CFI* and *IAASA*, respectively.

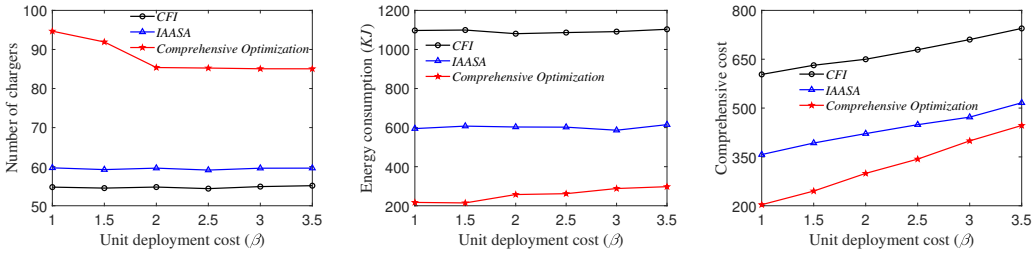

Fig. 10. Impact of unit deployment cost. (a) Number of chargers. (b) Energy consumption. (c) Comprehensive cost.

5.8 Comparison with Optimal Solution

We conduct a small-scale simulation in a square area $6m \times 6m$ to compare our algorithm with optimal solution of *CMCF* problem. In order to make the simulations more realistic, we change the coil radii from $0.1m$ to $0.08m$ and the energy capacity of charger from $150KJ$ to $30KJ$ to adapt to the small-scale environment. By enumerating all possible cases, we can find the optimal solution. Since the feasible solution must be a charging forest, the number of edges will not exceed $n-1$ when the number of sensor nodes is n. Given a graph $G(V,E)$, if there are h edges in the graph, the possible edges will only be selected from these edges. Thus, the maximum number of edges in the charging forest is $w = \min\{h, n-1\}$. Without considering the energy constraint, there are at most $\sum_{z=0,1,\ldots,w} \binom{h}{z}$ charging forests. For a certain forest with z edges, the number of chargers is $n-z$, and it is easy to find locations of the chargers to minimize the energy consumption of the charging forest in order to minimize the comprehensive cost of the charging forest. By enumerating all the cases, the optimal solution can be found from the feasible solutions, which satisfy the constraints. As shown in Fig. 11, We can see that our algorithm only increases 17.65% of the comprehensive cost comparing with *Optimal Solution* on average.

5.9 Running Time

We conduct the large-scale simulations to compare the running time of our algorithm with that of *CFI* and *IAASA* and the small-scale simulations to compare the running time of our algorithm with that of *Optimal Solution*. In the larger-scale simulations, we can see from Fig. 12(a) that our algorithm can output the solution in 0.85 seconds when there are 150 sensor nodes, thus shows great scalability. We can see from Fig. 12(b) that *Optimal Solution* takes 4.5 seconds even for 20 sensor nodes. On average, our algorithm reduces 71.08% of running time comparing with *Optimal Solution*.

6 DISCUSSION

In this section, we discuss some practical issues when implementing the multi-hop wireless charging, including charging scheduling, partial charging, and robustness.

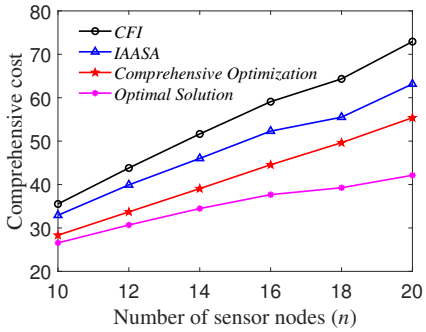

Fig. 11. Comparison with optimal solution.

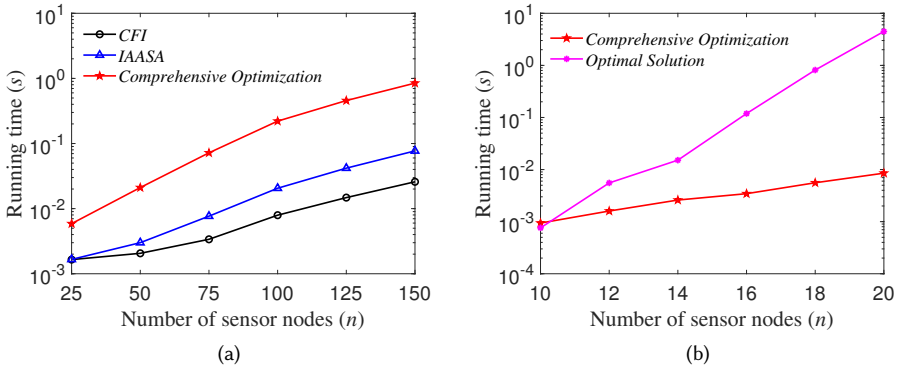

Fig. 12. Running time. (a) Large-scale simulations. (b) Small-scale simulations.

Charging scheduling. Although the multi-hop wireless charging may improve charging efficiency, it does not always deduces the charging time comparing with the single-hop wireless charging because the charging processing should be performed sequentially. Moreover, to avoid the "conflict" shown in Introduction section, some charging tasks cannot be performed simultaneously. Therefore, the charging schedule is needed in multi-hop wireless charging. Since the charging forest and the energy demand of each sensor node are known, it is possible to schedule the charging tasks and calculate the accurate charging time based on the designed schedule. A promising approach is to maintain a conflict graph for the transmitters which are ready to perform the charging tasks, and use the classic graph coloring algorithm [29] to select a set of transmitters with same color to perform the discharge tasks at each time. Another way is to employ the classic CSMA/CD [18] as the conflict detection protocol to avoid the "conflict". However, it is hard to calculate the accurate charging time if we use conflict detection protocol.

Partial charging. In our paper, the energy demands of all sensor nodes should be satisfied. Theoretically, the energy demand of each sensor node can be satisfied by partial charging of several times from multiple chargers using multi-hop wireless charging. We discuss the partial charging for our system model as follows: First, since the sensor nodes can be charged by multiple chargers, there will be overlap among charging trees, thus, the charger deployment is complicated; Second, although the energy cost could be reduced by partial charging, more charging trees are needed, thus, the

deployment cost increases. Therefore, the mixing of partial charging with multi-hop wireless charging is not always better than that with full charging in terms of comprehensive cost; Moreover, more charging trees aggravate the possible "conflict", thus, the charging scheduling is complicated, and more charging time is needed.

Robustness. Another important problem in actual charging is that some sensor nodes may fail. We cAnother important problem is the robustness in multi-hop wireless charging. When some sensor nodes fail to transfer energy, the energy demands of downstream sensor nodes cannot be fulfilled, thus, the self-recovery mechanism is necessary. When the failure happens, we can construct a new charging network as follows: The sensor nodes with more energy than their energy demands are regarded as chargers. The energy demands of sensor nodes whose energy demands are fulfilled are set as zero. The failure sensor nodes are removed from the charging network. Then we can perform the Charging Forest Initialization (Algorithm 1) to construct the charging forest based on the new charging network. An illustration of the self-recovery mechanism has been given in Fig. 13. Initially, there are two charging trees where the rectangles represent the roots of charging trees. We consider the failure happens at this moment, and then a new charging network is generated, where the yellow nodes represent the failure sensor nodes. The blue nodes represent the sensor nodes with more energy than their energy demands. The pink nodes represent the sensor nodes whose energy demands are fulfilled. The green nodes represent the sensor nodes whose energy demands are not fulfilled. Then a new charging forest based on the new charging network can be constructed through *Charging Forest Initialization*. Note that due to the existence of failure sensor nodes, some charging paths will be lost, thus, the energy demands of all sensor nodes may not be fully satisfied.

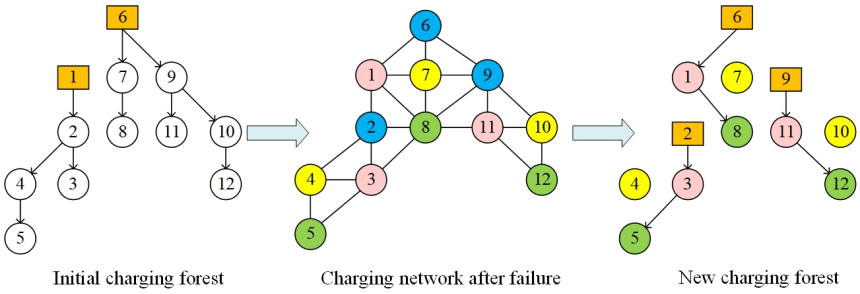

Fig. 13. Illustration of the self-recovery mechanism.

7 CONCLUSION

In this paper, we have defined a new metric, comprehensive cost, to measure the actual total economic cost for charger deployment in multi-hop wireless charging. We have presented a multi-hop wireless charging model and formulated the problem to minimize the comprehensive cost with energy capacity constraint of chargers. Due to the hardness of the original problem, we have designed a two-stage solution. The first stage aims to find the minimum number of chargers that can cover all sensor nodes with energy capacity constraint. We have proposed a greedy algorithm for the first stage. In the second stage, we have formulated the problem to maximize the reduction of comprehensive cost by adding chargers to the solution obtained from the first stage. We have shown that this problem is a submodular set function maximization problem in the unconstrained setting, which can be solved by a 1/2-approximation randomized linear time algorithm for its equivalent problem. Through extensive simulations, we demonstrate that the proposed

algorithm shows significant superiority in terms of comprehensive cost and can reduce the comprehensive cost by 57.55% comparing with the benchmark algorithms.

ACKNOWLEDGMENTS

This work has been supported in part by the National Natural Science Foundation of China (No. 61872193, 61872191, 62072254, 62272237) and the Graduate Student Scientific Research Innovation Projects in Jiangsu Province (KYCX22_1025) .

REFERENCES

[1] Ravindra Ahuja, James Orlin, Stefano Pallottino, Maria Scaparra, and Maria Scutellà. 2003. A Multi-Exchange Heuristic for the Single-Source Capacitated Facility Location Problem. *Management Science* 50 (02 2003), 749–760. https://doi.org/10.2139/ssrn.337621

[2] Niv Buchbinder, Moran Feldman, Joseph Naor, and Roy Schwartz. 2012. A Tight Linear Time (1/2)-Approximation for Unconstrained Submodular Maximization. In *2012 IEEE 53rd Annual Symposium on Foundations of Computer Science*. 649–658. https://doi.org/10.1109/FOCS.2012.73

[3] Woodbank Communications. 2005. *Battery Performance Characteristics*. Retrieved September 20, 2020 from https://www.mpoweruk.com/performance.htm

[4] Haipeng Dai, Ke Sun, Alex X. Liu, Lijun Zhang, Jiaqi Zheng, and Guihai Chen. 2021. Charging Task Scheduling for Directional Wireless Charger Networks. *IEEE Transactions on Mobile Computing* 20, 11 (2021), 3163–3180. https://doi.org/10.1109/TMC.2020.2997602

[5] Uriel Feige. 1998. A Threshold of Ln n for Approximating Set Cover. *J. ACM* 45, 4 (jul 1998), 634–652. https://doi.org/10.1145/285055.285059

[6] Tian Hao, Ruogu Zhou, Guoliang Xing, Matt W. Mutka, and Jiming Chen. 2014. WizSync: Exploiting Wi-Fi Infrastructure for Clock Synchronization in Wireless Sensor Networks. *IEEE Transactions on Mobile Computing* 13, 6 (2014), 1379–1392. https://doi.org/10.1109/TMC.2013.43

[7] Yong Jin, Jia Xu, Sixu Wu, Lijie Xu, and Dejun Yang. 2021. Enabling the Wireless Charging via Bus Network: Route Scheduling for Electric Vehicles. *IEEE Transactions on Intelligent Transportation Systems* 22, 3 (2021), 1827–1839. https://doi.org/10.1109/TITS.2020.3023695

[8] Yong Jin, Jia Xu, Sixu Wu, Lijie Xu, Dejun Yang, and Kaijian Xia. 2021. Bus network assisted drone scheduling for sustainable charging of wireless rechargeable sensor network. *Journal of Systems Architecture* 116 (2021). https://doi.org/10.1016/j.sysarc.2021.102059

[9] Vladimir Kindl, Roman Pechanek, Martin Zavrel, and Tomas Kavalir. 2018. Inductive coupling system for E-bike wireless charging. In *2018 ELEKTRO*. 1–4. https://doi.org/10.1109/ELEKTRO.2018.8398268

[10] Brian J. Lee, Andrew Hillenius, and David S. Ricketts. 2012. Magnetic resonant wireless power delivery for distributed sensor and wireless systems. In *2012 IEEE Topical Conference on Wireless Sensors and Sensor Networks*. 13–16. https://doi.org/10.1109/WiSNet.2012.6172148

[11] Christoph Lenzen, Philipp Sommer, and Roger Wattenhofer. 2009. Optimal Clock Synchronization in Networks. In *Proceedings of the 7th ACM Conference on Embedded Networked Sensor Systems*. Association for Computing Machinery, New York, NY, USA, 225–238. https://doi.org/10.1145/1644038.1644061

[12] Shuo Li, Jian He, Xiaoyong Zhang, and Jun Peng. 2015. An Energy Efficient Multi-hop Charging Scheme with Mobile Charger for Wireless Rechargeable Sensor Network. In *Algorithms and Architectures for Parallel Processing*, Guojun Wang, Albert Zomaya, Gregorio Martinez, and Kenli Li (Eds.). Springer International Publishing, Cham, 648–660. https://doi.org/10.1007/978-3-319-27119-4_45

[13] Chi Lin, Feng Gao, Haipeng Dai, Lei Wang, and Guowei Wu. 2019. When Wireless Charging Meets Fresnel Zones: Even Obstacles Can Enhance Charging Efficiency. In *2019 16th Annual IEEE International Conference on Sensing, Communication, and Networking (SECON)*. 1–9. https://doi.org/10.1109/SAHCN.2019.8824816

[14] Chi Lin, Wei Yang, Haipeng Dai, Teng Li, Yi Wang, Lei Wang, Guowei Wu, and Qiang Zhang. 2021. Near Optimal Charging Schedule for 3-D Wireless Rechargeable Sensor Networks. *IEEE Transactions on Mobile Computing* (2021), 1–1. https://doi.org/10.1109/TMC.2021.3137308

[15] Chi Lin, Ziwei Yang, Haipeng Dai, Liangxian Cui, Lei Wang, and Guowei Wu. 2021. Minimizing Charging Delay for Directional Charging. *IEEE/ACM Transactions on Networking* 29, 6 (2021), 2478–2493. https://doi.org/10.1109/TNET.2021.3095280

[16] Tang Liu, Baijun Wu, Shihao Zhang, Jian Peng, and Wenzheng Xu. 2020. An Effective Multi-node Charging Scheme for Wireless Rechargeable Sensor Networks. In *IEEE INFOCOM 2020 - IEEE Conference on Computer Communications*. 2026–2035. https://doi.org/10.1109/INFOCOM41043.2020.9155262

[17] Xiao Lu, Ping Wang, Dusit Niyato, Dong In Kim, and Zhu Han. 2016. Wireless Charging Technologies: Fundamentals, Standards, and Network Applications. *IEEE Communications Surveys & Tutorials* 18, 2 (2016), 1413–1452. https://doi.org/10.1109/COMST.2015.2499783

[18] J. Meditch and Chin-Tan Lea. 1983. Stability and Optimization of the CSMA and CSMA/CD Channels. *IEEE Transactions on Communications* 31, 6 (1983), 763–774. https://doi.org/10.1109/TCOM.1983.1095881

[19] Jose Oscar Mur-Miranda, Giulia Fanti, Yifei Feng, Keerthik Omanakuttan, Roydan Ongie, Albert Setjoadi, and Natalie Sharpe. 2010. Wireless power transfer using weakly coupled magnetostatic resonators. In *2010 IEEE Energy Conversion Congress and Exposition*. 4179–4186. https://doi.org/10.1109/ECCE.2010.5617728

[20] Smriti Priyadarshani, Abhinav Tomar, and Prasanta K. Jana. 2021. An efficient partial charging scheme using multiple mobile chargers in wireless rechargeable sensor networks. *Ad Hoc Networks* 113 (2021), 102407. https://doi.org/10.1016/j.adhoc.2020.102407

[21] Tifenn Rault, Abdelmadjid Bouabdallah, and Yacine Challal. 2013. Multi-hop wireless charging optimization in low-power networks. In *2013 IEEE Global Communications Conference (GLOBECOM)*. 462–467. https://doi.org/10.1109/GLOCOM.2013.6831114

[22] A. V. Sutar, Vanita Dighe, Prathamesh Karavkar, Piyusha Mhatre, and Vijaya Tandel. 2020. Solar Energy based Mobile Charger Using Inductive Coupling Transmission. In *2020 4th International Conference on Intelligent Computing and Control Systems (ICICCS)*. 995–1000. https://doi.org/10.1109/ICICCS48265.2020.9120916

[23] Abhinav Tomar and Prasanta K. Jana. 2021. A multi-attribute decision making approach for on-demand charging scheduling in wireless rechargeable sensor networks. *Computing* 103 (2021), 1677–1701. https://doi.org/10.1007/s00607-020-00875-w

[24] Suda Tragantalerngsak, John Holt, and Mikael Rönnqvist. 2000. An exact method for the two-echelon, single-source, capacitated facility location problem. *European Journal of Operational Research* 123, 3 (2000), 473–489. https://doi.org/10.1016/S0377-2217(99)00105-8

[25] Cong Wang, Ji Li, Fan Ye, and Yuanyuan Yang. 2017. A Novel Framework of Multi-Hop Wireless Charging for Sensor Networks Using Resonant Repeaters. *IEEE Transactions on Mobile Computing* 16, 3 (2017), 617–633. https://doi.org/10.1109/TMC.2016.2567382

[26] Ning Wang, Jie Wu, and Haipeng Dai. 2019. Bundle Charging: Wireless Charging Energy Minimization in Dense Wireless Sensor Networks. In *2019 IEEE 39th International Conference on Distributed Computing Systems (ICDCS)*. 810–820. https://doi.org/10.1109/ICDCS.2019.00085

[27] Mohamed K. Watfa, Haitham Al-Hassanieh, and Samir Salmen. 2008. The road to immortal sensor nodes. In *2008 International Conference on Intelligent Sensors, Sensor Networks and Information Processing*. 523–528. https://doi.org/10.1109/ISSNIP.2008.4762042

[28] Mohamed K. Watfa, Haitham AlHassanieh, and Samir Selman. 2011. Multi-Hop Wireless Energy Transfer in WSNs. *IEEE Communications Letters* 15, 12 (2011), 1275–1277. https://doi.org/10.1109/LCOMM.2011.092911.100129

[29] D. J. A. Welsh and M. B. Powell. 1967. An upper bound for the chromatic number of a graph and its application to timetabling problems. *Comput. J.* 10, 1 (1967), 85–86. https://doi.org/10.1093/comjnl/10.1.85

[30] WiTricity. 2015. *Witricity Leverages Magnetic Resonance for Flexible Wireless Charging*. Retrieved October 25, 2019 from https://cn.comsol.com/story/download/350121/WiTricity_MS15.pdf

[31] Sixu Wu, Haipeng Dai, Linfeng Liu, Lijie Xu, Fu Xiao, and Jia Xu. 2022. Cooperative Scheduling for Directional Wireless Charging with Spatial Occupation. *IEEE Transactions on Mobile Computing* (2022), 1–16. https://doi.org/10.1109/TMC.2022.3214979

[32] Yuan Wu, Yong Feng, Lei Guo, and Xin Yang. 2018. Deployment Method for Resonant Repeaters in Multi-hop Wireless Rechargeable Sensor Networks. *Transducer and Microsystem Technologies* 37 (2018), 42–45+48. http://en.cnki.com.cn/Article_en/CJFDTotal-CGQJ201812012.htm

[33] Jia Xu, Suyi Hu, Sixu Wu, Kaijun Zhou, Haipeng Dai, and Lijie Xu. 2021. Cooperative Charging as Service: Scheduling for Mobile Wireless Rechargeable Sensor Networks. In *2021 IEEE 41st International Conference on Distributed Computing Systems (ICDCS)*. 685–695. https://doi.org/10.1109/ICDCS51616.2021.00071

[34] Lijie Xu, Haodong Sha, Mingxiang Da, Jia Xu, and Haipeng Dai. 2022. Spatio-Temporal Mobile Cooperative Charging for Low-Power Wireless Rechargeable Devices. In *IEEE International Conference on Mobile Ad-Hoc and Smart Systems*. 1–9.

[35] W. X. Zhong, Chi Kwan Lee, and S. Y. Hui. 2012. Wireless power domino-resonator systems with noncoaxial axes and circular structures. *IEEE Transactions on Power Electronics* 27, 11 (2012), 4750–4762. https://doi.org/10.1109/TPEL.2011.2174655

[36] Pengzhan Zhou, Cong Wang, and Yuanyuan Yang. 2019. Static and Mobile Target k-Coverage in Wireless Rechargeable Sensor Networks. *IEEE Transactions on Mobile Computing* 18, 10 (2019), 2430–2445. https://doi.org/10.1109/TMC.2018.2872576